JACS
JOURNAL OF THE AMERICAN CHEMICAL SOCIETY
pubs.acs.org/JACS
Article

Identifying Sources of Entanglement Loss in Photodriven Molecular Electron Spin Teleportation

Yuheng Huang, Yunfan Qiu, Ryan M. Young, George C. Schatz,* Matthew D. Krzyaniak,* and Michael R. Wasielewski*

Cite This: J. Am. Chem. Soc. 2024, 146, 20133−20140
Read Online
ACCESS | Metrics & More | Article Recommendations | Supporting Information

ABSTRACT: We report on an electron donor-electron acceptor-stable radical (D-A-R$^{\bullet}$) molecule in which an electron spin state first prepared on R$^{\bullet}$ is followed by photogeneration of an entangled singlet ^{1}[D$^{\bullet+}$-A$^{\bullet-}$] spin pair to produce D$^{\bullet+}$-A$^{\bullet-}$-R$^{\bullet}$. Since the A$^{\bullet-}$ and R$^{\bullet}$ spins within D$^{\bullet+}$-A$^{\bullet-}$-R$^{\bullet}$ are uncorrelated, spin teleportation from R$^{\bullet}$ to D$^{\bullet+}$ occurs with a maximal 25% efficiency only for the singlet pair ^{1}(A$^{\bullet-}$-R$^{\bullet}$) by spin-allowed electron transfer from A$^{\bullet-}$ to R$^{\bullet}$. However, since ^{1}[D$^{\bullet+}$-A$^{\bullet-}$] is sufficiently long-lived, coherent spin mixing involving the unreactive ^{3}(A$^{\bullet-}$-R$^{\bullet}$) population affects entanglement and teleportation within D$^{\bullet+}$-A$^{\bullet-}$-R$^{\bullet}$. Pulse electron paramagnetic resonance experiments show a direct correlation between electron spin flip-flops and entanglement loss, providing information for designing molecular materials to serve as nanoscale quantum device interconnects.

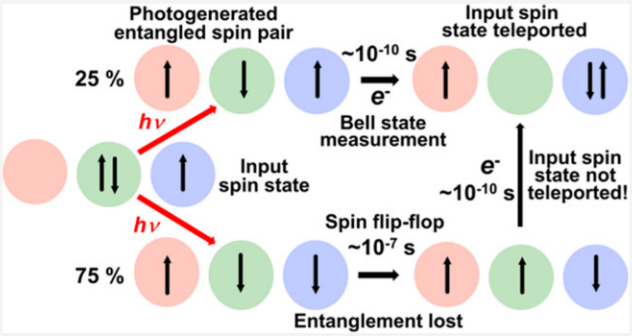

INTRODUCTION

Quantum teleportation is widely regarded as essential to quantum communications because it provides a way to bypass the no-cloning theorem that precludes copying an arbitrary quantum state.[1−5] The three decades following Bennett's original proposal of quantum teleportation have seen the physical realization of this protocol on numerous platforms, with teleported states ranging from discrete- and continuous-variable photonic states to quantum states encoded in superconducting transmon qubits.[6−16] Factors that dictate the utility of teleportation procedures include entanglement generation,[17−19] coherence time,[20−22] Bell state measurement (BSM) efficiency,[7,11,19,23,24] and fidelity.[25,26]

In previous work, we reported a teleportation scheme mediated through photoinitiated ultrafast electron transfer within an ensemble of linear, covalent electron donor-electron acceptor-stable radical (D-A-R$^{\bullet}$) molecules,[27,28] in which an electron spin state is first prepared on R$^{\bullet}$ using a resonant microwave pulse. This pulse is immediately followed by a laser pulse that selectively excites the electron acceptor/chromophore (A) within a covalent D-A-R$^{\bullet}$ molecule to its lowest singlet excited state, which results in ultrafast ($\sim 10^{11}$ s^{-1}) electron transfer from D to A yielding a spin-entangled singlet D$^{\bullet+}$-A$^{\bullet-}$ pair in near unity yield, where D$^{\bullet+}$ and A$^{\bullet-}$ as well as A$^{\bullet-}$ and R$^{\bullet}$ are strongly exchange coupled, while the coupling between D$^{\bullet+}$ and R$^{\bullet}$ is negligible. To distinguish between the spin pair states, we label the D$^{\bullet+}$-A$^{\bullet-}$ states with square brackets and the A$^{\bullet-}$-R$^{\bullet}$ states with parentheses. The purity of the initially entangled ^{1}[D$^{\bullet+}$-A$^{\bullet-}$] state is nearly unity, even at room temperature, matching processes that depend on more demanding system architectures and mK temperatures, such as superconducting circuits and trapped neutral atoms or ions.[6,9,13,29] The subsequent energetically favorable electron transfer ^{1}[D$^{\bullet+}$-^{1}(A$^{\bullet-}$]-R$^{\bullet}$) → D$^{\bullet+}$-A-R$^-$ only occurs for the ^{1}(A$^{\bullet-}$-R$^{\bullet}$) singlet subensemble, i.e., $|S\rangle = \frac{1}{\sqrt{2}}(|\uparrow\downarrow\rangle - |\downarrow\uparrow\rangle$, and constitutes a conditional Bell state measurement (BSM) with a maximal 25% efficiency. In the reported case, a second microwave pulse that is resonant with D$^{\bullet+}$ was used to read out the state teleported to D$^{\bullet+}$.[27,28] Tailoring such molecular spin teleportation systems affords the possibility of using molecular assemblies to conduct coherent information transfer over the nanometers to tens of nanometers length scales required for quantum device interconnects.[30]

Our original D-A-R$^{\bullet}$ molecule exhibits a 90% teleportation fidelity for the 25% singlet subensemble ^{1}[D$^{\bullet+}$-^{1}(A$^{\bullet-}$]-R$^{\bullet}$),[27] and its design ensures that ^{1}[D$^{\bullet+}$-A$^{\bullet-}$] recombination to the ground state is sufficiently rapid to eliminate the corresponding 75% triplet subensemble ^{1}[D$^{\bullet+}$-^{3}(A$^{\bullet-}$]-R$^{\bullet}$) that cannot

Received: March 29, 2024
Revised: June 26, 2024
Accepted: June 27, 2024
Published: July 12, 2024

https://doi.org/10.1021/jacs.4c04393
J. Am. Chem. Soc. 2024, 146, 20133−20140

produce $D^{\bullet+}$-A-R^{-} prior to read out of the spin state teleported to $D^{\bullet+}$.[27] In this article, we examine a new D-A-$R^{\bullet}$ molecule in which the $^1[D^{\bullet+}\text{-}A^{\bullet-}]$ recombination rate is slow enough to allow a $^1[D^{\bullet+}\text{-}^3(A^{\bullet-})\text{-}R^{\bullet}) \rightarrow {}^3[D^{\bullet+}\text{-}^1(A^{\bullet-})\text{-}R^{\bullet})$ spin flip-flop to occur, which results in delayed formation of a second $^1(A^{\bullet-}\text{-}R^{\bullet})$ population that also engages in the reaction $^3[D^{\bullet+}\text{-}^1(A^{\bullet-})\text{-}R^{\bullet}) \rightarrow D^{\bullet+}\text{-A-}R^{-}$. Since this spin flip-flop could result in entanglement loss within the photogenerated $^1[D^{\bullet+}\text{-}A^{\bullet-}]$ Bell pair, we use pulse electron paramagnetic resonance techniques to probe the spin dynamics of the $^3(A^{\bullet-}\text{-}R^{\bullet})$ subensemble and evaluate $^1[D^{\bullet+}\text{-}A^{\bullet-}]$ entanglement loss based on whether spin information can be successfully recovered after the spin flip-flop occurs.[31]

To probe these phenomena, we have prepared the D-A-$R^{\bullet}$ system shown in Figure 1a, where D is tetrathiofulvalene

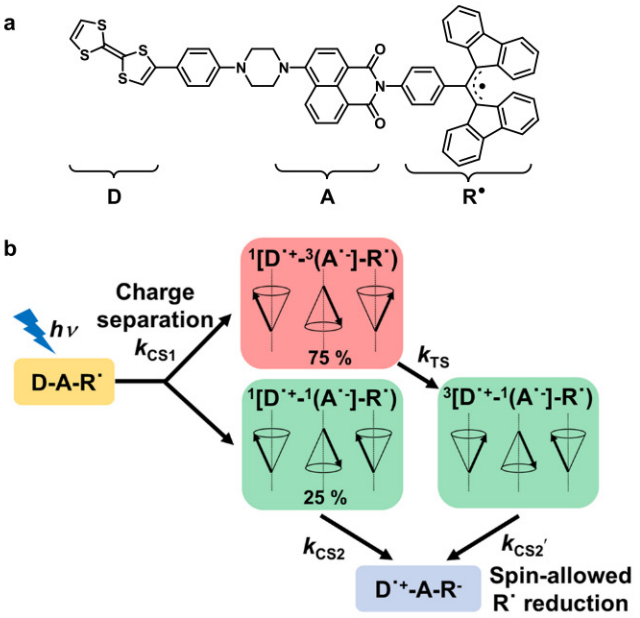

Figure 1. (a) Chemical structure of D-A-$R^{\bullet}$. (b) Relevant states and rate constants for their formation. Square brackets and parentheses were used to differentiate spin configurations. Upon charge separation, subensembles $^1[D^{\bullet+}\text{-}^1(A^{\bullet-})\text{-}R^{\bullet})$ and $^1[D^{\bullet+}\text{-}^3(A^{\bullet-})\text{-}R^{\bullet})$ are populated stochastically. The simplified vector diagram depicts the spin flip-flop motion, where only the T_0 states at high magnetic fields are depicted. Analogous vector diagrams can be drawn for the $T_{\pm1}$ states. Configurations that satisfy the spin-selective rules (green boxes) can undergo energetically favorable Ṙ reduction. Complete energetics are shown in Figure S1.

(TTF), A is 4-aminonaphthalene-1,8-imide (ANI), and $R^{\bullet}$ is partially deuterated α,γ-bisdiphenylene-β-phenylallyl (BDPA) (see the Supporting Information). Since entanglement is essential for quantum teleportation,[4] certifying whether entanglement is maintained in this system requires differentiating between the two subensembles described above. By burning a spectral hole in the initial state of $R^{\bullet}$, we are able to access essential information regarding these spin dynamics, which informs system design criteria for teleportation at a length scale underexplored for electron spin qubits.[32] With this information in hand, reducing the ensembles to the single-molecule level can be envisioned, where photoluminescence from a suitable D-A-$R^{\bullet}$ system or an auxiliary luminescent probe can be used to read out the teleported quantum state.

RESULTS AND DISCUSSION

Electron Transfer Dynamics. Figures 1b and S2 show the electron transfer pathways possible for the photogenerated three-spin system described above.[27,28] Through careful selection of the system building blocks, we can eliminate pathways irrelevant to Bell state measurement. As noted above, the initial spin configuration between acceptor $A^{\bullet-}$ and stable radical $R^{\bullet}$ is purely stochastic upon rapid formation of $D^{\bullet+}\text{-}A^{\bullet-}\text{-}R^{\bullet}$, resulting in 25% $^1[D^{\bullet+}\text{-}^1(A^{\bullet-})\text{-}R^{\bullet})$ and 75% $^1[D^{\bullet+}\text{-}^3(A^{\bullet-})\text{-}R^{\bullet})$. It is immediately obvious that additional spin dynamics may be possible if the intersystem crossing rate k_{TS} is on the same order of magnitude as the decay rate of $^1[D^{\bullet+}\text{-}A^{\bullet-}] \rightarrow {}^1[D\text{-}A]$. In the following sections, we will show direct experimental evidence supporting this assertion.

The ground-state electronic absorption spectrum of D-A-$R^{\bullet}$ has bands characteristic of the chromophore/acceptor A and the stable radical $R^{\bullet}$ at 400 and 490 nm, respectively (Figure 2a).[27] Transient optical absorption measurements were conducted on D-A-$R^{\bullet}$ in a butyronitrile glass at 85 K to characterize the charge transfer dynamics of D-A-$R^{\bullet}$ following selective photoexcitation of A with a 414 nm laser pulse. Donor D and stable radical $R^{\bullet}$ were selected such that following photoexcitation of A, the charge separation D-^{1}*A-$R^{\bullet} \rightarrow D^{\bullet+}\text{-}A^{\bullet-}\text{-}R^{\bullet}$ and subsequent radical reduction $D^{\bullet+}\text{-}A^{\bullet-}\text{-}R^{\bullet} \rightarrow D^{\bullet+}\text{-A-}R^{-}$ reactions are energetically favorable (see the Supporting Information). The formation of $D^{\bullet+}\text{-}A^{\bullet-}\text{-}R^{\bullet}$ occurs with $k_{CS1} = (1.0 \pm 0.3) \times 10^{11}$ s^{-1}, as indicated by the disappearance of stimulated emission from ^{1}*A at 520 nm and concurrent emergence of the signature feature of $A^{\bullet-}$ at 430 nm (Figure 2b,c).[27] Reduction of $R^{\bullet}$ is evidenced by the ground-state bleach of $R^{\bullet}$ at 490 nm and formation of the absorption of R^{-} at 620 nm with $k_{CS2} = (7.2 \pm 0.2) \times 10^9$ s^{-1} (Figure 2b,c). A species with spectral features identical to R^{-} emerges later at a much slower rate $k_{CS2'} = (6.6 \pm 0.3) \times 10^6$ s^{-1}. The three-order-of-magnitude rate difference between k_{CS2} and $k_{CS2'}$ is interpreted as resulting from a slow spin flip-flop, $^1[D^{\bullet+}\text{-}^3(A^{\bullet-})\text{-}R^{\bullet}) \rightarrow {}^3[D^{\bullet+}\text{-}^1(A^{\bullet-})\text{-}R^{\bullet})$, followed by a fast spin-allowed radical reduction. The $D^{\bullet+}\text{-A-}R^{-}$ product decays with $k_{CR2} = (1.0 \pm 0.2) \times 10^5$ s^{-1}, allowing for EPR detection of the $D^{\bullet+}$ populations produced by both processes. Additional transient optical data is presented in the Supporting Information.

Spin Dynamics. A delay-after-flash EPR experiment was conducted with a variable delay time (τ_{DAF}) between the laser pulse and the broadband, nonselective Hahn-echo microwave pulse sequence ($\pi/2\text{-}\tau\text{-}\pi$), where τ is the delay between the $\pi/2$ and π pulses (Figure 3a and the Supporting Information). The EPR spectra in the frequency domain were obtained by recording the entire spin echo trace in the time domain at the central magnetic field of the spectrum and performing a Fourier transform.[33] The bandwidth of the microwave pulses was held constant, and the tip angle of the magnetization was determined by the amplitudes of the pulses. The light-minus-dark difference spectra observed for both $R^{\bullet}$ and $D^{\bullet+}$ at τ_{DAF} = 1 μs following selective photoexcitation of A in D-A-$R^{\bullet}$ are well-separated because of their large g-tensor difference (Figure 3b).[34] Since the spin−spin exchange coupling between $D^{\bullet+}$ and $A^{\bullet-}$ within photogenerated $D^{\bullet+}\text{-}A^{\bullet-}$ is large (see below), the only reaction product detectable by EPR is $D^{\bullet+}\text{-A-}R^{-}$.[35,36] Based on population changes alone, the decrease in the $R^{\bullet}$ signal is expected; however, this should be accompanied by the appearance of a positive $D^{\bullet+}$ signal following the D-^{1}*A-$R^{\bullet} \rightarrow$

https://doi.org/10.1021/jacs.4c04393
J. Am. Chem. Soc. 2024, 146, 20133−20140

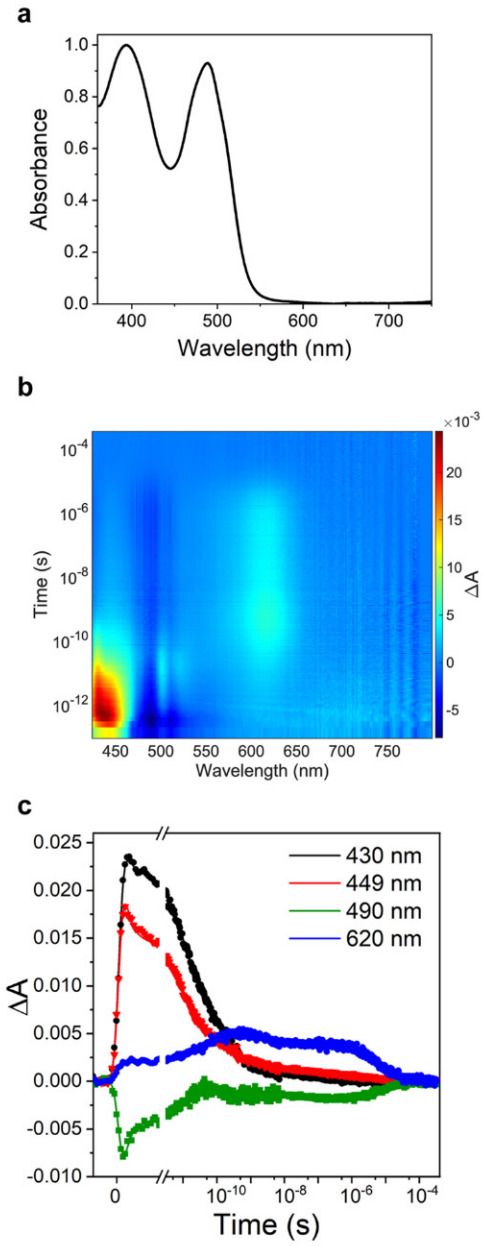

Figure 2. (a) Optical absorption spectrum of D-A-R$^{\bullet}$. (b) Plot of ΔA vs time and wavelength following selective photoexcitation of acceptor A within D-A-R$^{\bullet}$ in PrCN at 85 K with 414 nm laser pulses. (c) Time dependence of ΔA at selected wavelengths and the corresponding kinetic fits (see Supporting Information).

$^1[D^{\bullet+}\text{-}^1(A^{\bullet-})\text{-}R^{\bullet}]$ → $D^{\bullet+}$-A-R^- charge transfer sequence. However, the $D^{\bullet+}$ signal in the observed difference spectra (Figure 3c) is also negative and appears relatively slowly with rate constant $k_A = (6.6 \pm 0.3) \times 10^6$ s^{-1} (Figure 3d). This is attributed to spin polarization of $D^{\bullet+}$ resulting from the slow spin flip-flop $^1[D^{\bullet+}\text{-}^3(A^{\bullet-})\text{-}R^{\bullet}]$ → $^3[D^{\bullet+}\text{-}^1(A^{\bullet-})\text{-}R^{\bullet}]$, which is necessary for the second, delayed, spin-allowed electron transfer $^1(A^{\bullet-}\text{-}R^{\bullet})$ → (A-R^-) to occur. The $D^{\bullet+}$ signal decays with rate constant $k_D = (1.4 \pm 0.2) \times 10^5$ s^{-1} (Figure 3d).

Although intersystem crossing in biradicals typically occurs in hundreds of nanoseconds,[37−39] consistent with the rate reported here, its mechanism and effect on entanglement in a three-spin system have yet to be thoroughly explored. Assuming J_{DR} is small,[40] the $^1[D^{\bullet+}\text{-}^3(A^{\bullet-})\text{-}R^{\bullet}]$ → $^3[D^{\bullet+}\text{-}^1(A^{\bullet-})\text{-}R^{\bullet})$ spin flip-flop, which we distinguish from pairwise flip-flops typical of coupled spin relaxations, is hypothesized to be driven by the spin−spin exchange interactions J_{DA} and J_{AR}. Since charge recombination of $^1[D^{\bullet+}\text{-}A^{\bullet-}]$ → D−A in the D-A-RH reference molecule occurs in $\tau \sim 50$ ns, using the free energy of reaction and the total nuclear reorganization energy for recombination, the electronic coupling matrix element for charge recombination calculated using Marcus-Jortner electron transfer theory[41,42] is V_{DA} = 16 cm^{-1} (see the Supporting Information). Further, using V_{DA} in the second-order perturbation treatment of Kobori et al.,[43] we estimate $J_{DA} \cong 0.7$ GHz. Using the same methodology, we derive V_{AR} = 37 cm^{-1} from the $D^{\bullet+}\text{-}A^{\bullet-}\text{-}R^{\bullet}$ → $D^{\bullet+}$-A-R^- electron transfer process so that $J_{AR} \cong 32$ GHz, which agrees with previous estimates.[44,45]

In a three-spin system with two pairs of strongly exchange coupled spins, the singlet−triplet basis for either pair is no longer a good eigenbasis for its spin Hamiltonian. This directly results in an initial population involving mixed states (Supporting Information Section 6). Kandrashkin explored the singlet−triplet decoherence within $[D^{\bullet+}\text{-}A^{\bullet-}]$ of such a system in the fast-decay limit and suggested that an enhanced quantum yield of $D^{\bullet+}$-A-R^- is conceivable.[46] For $^1[D^{\bullet+}\text{-}^3(A^{\bullet-})\text{-}R^{\bullet}]$ reported here, which has no rapid decay pathway, coherent state mixing can readily occur due to the mixed characters of the initial states and can be modeled using a stochastic Liouville treatment (Supporting Information Section 6). This spontaneous state mixing needs to obey spin conservation such that m_S remains constant and is physically pictured by our proposed spin flip-flop. The exchange-mediated spin flip-flop motion can preferentially mix certain eigenstates of the total system Hamiltonian, giving rise to polarization of stable radical $R^{\bullet}$ (Supporting Information Section 6). Throughout this mixing process, bipartite entanglement within the initial $^1[D^{\bullet+}\text{-}A^{\bullet-}]$ state may be lost because the initial correlation between the pair can be distributed across all three spins via exchange interactions.[47] If this is the case, preparing a specific $R^{\bullet}$ input state should have no effect on the $D^{\bullet+}$ output spin state, although spin polarization can occur. Therefore, the Rabi oscillation experiments discussed below evaluate the efficacy of teleportation, as well as allow for direct observation of entanglement loss.

Teleportation Via the Singlet Spin Subensemble. To certify that teleportation occurs in the $^1[D^{\bullet+}\text{-}^1(A^{\bullet-})\text{-}R^{\bullet}]$ subensemble, we conducted Rabi oscillation experiments (Figure 4a). In both experiments, a variable length nutation pulse (τ_{NUT}) resonant with $R^{\bullet}$ was used to prepare the input spin state. The spin states were measured using broadband, nonselective Hahn-echo detection pulses. The Rabi oscillations of $R^{\bullet}$ in the absence of photoexcitation are shown in Figure 4c, black trace. The second experiment was conducted in an identical manner except that the laser pulse was applied at τ_{DAF} = 1 μs to produce $^1[D^{\bullet+}\text{-}A^{\bullet-}]$. The observed Rabi oscillations of the $D^{\bullet+}$ output state signal are convolved with a net emissive signal (Figure 4c, blue trace). The $D^{\bullet+}$ output signal Rabi oscillations were deconvolved from the net emissive signal, normalized, and compared to the oscillations observed for the $R^{\bullet}$ input state (Figure 4c, red and black traces). The oscillations of the $R^{\bullet}$ input and the $D^{\bullet+}$ output states occur with the same frequency and phase, indicating successful teleportation of the $R^{\bullet}$ spin state to $D^{\bullet+}$. In the meantime, the emissive signal remains constant irrespective of the nutation pulse length τ_{NUT}. This is attributed to the spin flip-flop

https://doi.org/10.1021/jacs.4c04393
J. Am. Chem. Soc. 2024, 146, 20133−20140

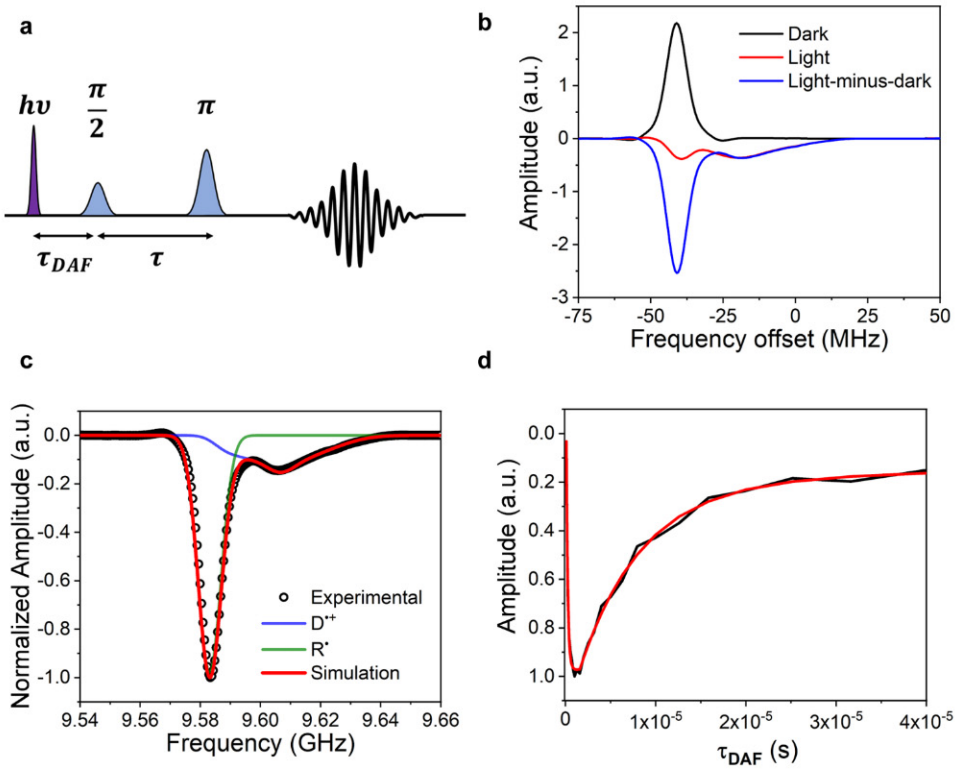

Figure 3. (a) Pulse sequence used to obtain the time-domain EPR spectra. Acceptor A in D-A-R$^{\bullet}$ dissolved in a PrCN glass at 85 K was selectively photoexcited using 417 nm, 7 ns laser pulses. The pulse parameters and signal processing methodologies are summarized in the Supporting Information. (b) Frequency domain spectra obtained by Fourier-transformation of the time domain Hahn echoes obtained at τ_{DAF} = 1 μs. (c) Simulation of the light-minus-dark difference spectrum. (d) Kinetic trace that monitors the population of D$^{\bullet+}$.

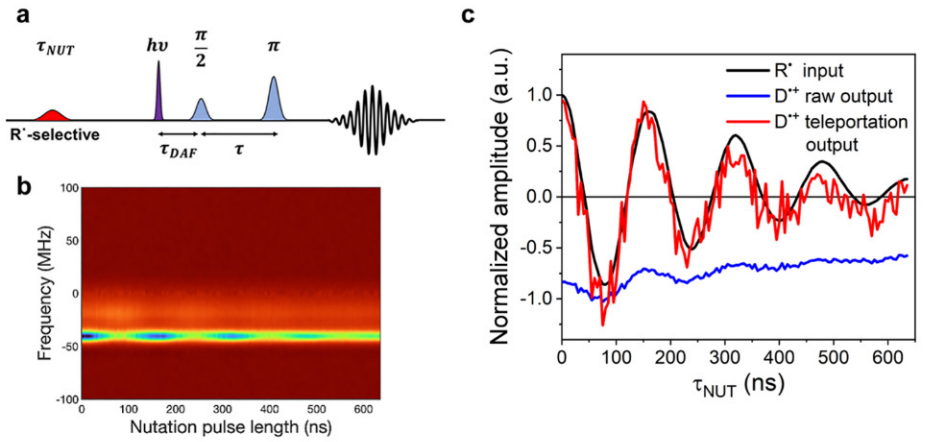

Figure 4. (a) Pulse sequence of the teleportation experiment. (b) Amplitude of the Rabi oscillations vs oscillation frequency and nutation pulse length. (c) Black trace shows Rabi oscillations of R$^{\bullet}$ following the pulse sequence shown in panel (a) without the laser pulse and all microwave pulses resonant with R$^{\bullet}$. The blue trace shows Rabi oscillations following the pulse sequence shown in panel (a) with the laser pulse applied, where the nutation pulse is resonant with R$^{\bullet}$ and the Hahn-echo pulse sequence is resonant with the D$^{\bullet+}$ output state. The blue trace is the raw signal amplitude in which the emissive hyperpolarization of D$^{\bullet+}$ constitutes a background signal convolved with the Rabi oscillations of D$^{\bullet+}$ resulting from teleportation of the spin state of R$^{\bullet}$ to D$^{\bullet+}$. The red trace is the teleportation signal from D$^{\bullet+}$ after subtraction of the hyperpolarization background and normalization to the R$^{\bullet}$ input signal.

occurring within ^{1}[D$^{\bullet+}$-^{3}(A$^{\bullet-}$)-R$^{\bullet}$) and is further investigated in the following section.

Differentiating between Singlet and Triplet Spin Subensembles. A suite of pulse-EPR experiments were designed to distinguish between the ^{1}[D$^{\bullet+}$-^{1}(A$^{\bullet-}$)-R$^{\bullet}$) and ^{1}[D$^{\bullet+}$-^{3}(A$^{\bullet-}$)-R$^{\bullet}$) subensembles by preparing a specific initial spin state of R$^{\bullet}$ prior to photogeneration of ^{1}[D$^{\bullet+}$-A$^{\bullet-}$]. First, the effect of the triplet subensemble spin dynamics on the EPR spectrum can be studied by eliminating the contribution from the singlet subensemble. Applying a sequence of 10 π/2 pulses spaced 1 μs apart to D-A-R$^{\bullet}$ saturates the initial Boltzmann-populated electron spin state of R$^{\bullet}$ (Figure 5a). When this is followed by a laser pulse to create D$^{\bullet+}$-A$^{\bullet-}$-R$^{\bullet}$ and a subsequent Hahn-echo detection pulse sequence probing D$^{\bullet+}$, there should be no spin echo from D$^{\bullet+}$ produced from the teleportation event ^{1}[D$^{\bullet+}$-^{1}(A$^{\bullet-}$)-R$^{\bullet}$) → D$^{\bullet+}$-A-R^{-} because

https://doi.org/10.1021/jacs.4c04393
J. Am. Chem. Soc. 2024, 146, 20133−20140

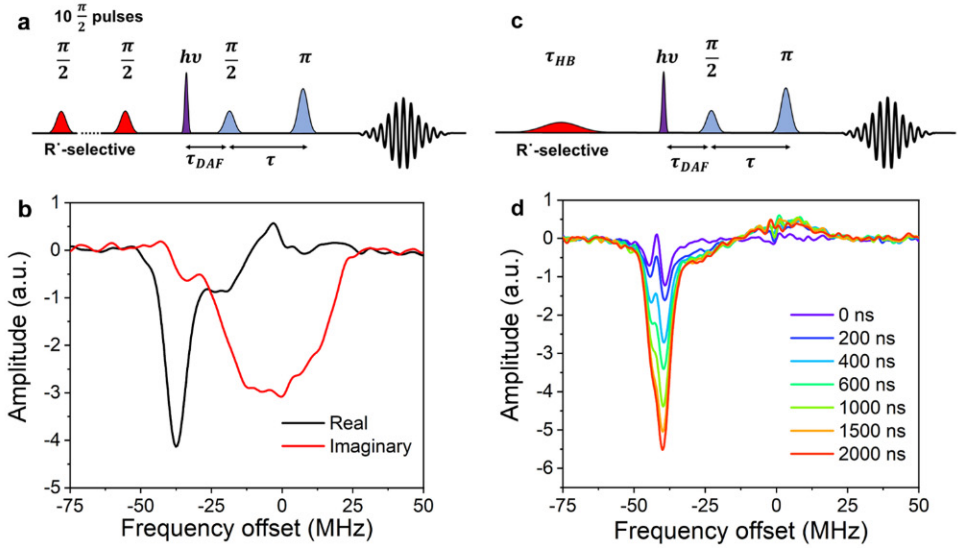

Figure 5. (a) Pulse sequence for the picket-fence pulse experiment. (b) EPR spectrum following photoexcitation of acceptor A in D-A-R$^{\bullet}$ in PrCN with 417 nm, 7 ns laser pulses after a series of picket-fence presaturation pulses are applied to R$^{\bullet}$. The presaturation sequence comprises 10 $\pi/2$ pulses spaced 1 μs apart from each other. Due to limited excitation bandwidth of the microwave pulses, signals from R$^{\bullet}$ and D$^{\bullet+}$ were refocused into the real and imaginary quadrature channels, respectively. (c) Pulse sequence for the hole-burning experiment. A low-power, narrow-bandwidth, R$^{\bullet}$-selective pulse with a turning angle of $\sim 5\pi$ was used to achieve optimal hole burning. (d) Delay-after-flash EPR experiment conducted after a spectral hole was burned into R$^{\bullet}$.

there is no net magnetization on R$^{\bullet}$ (Figure S7). This is not true for ^{1}[D$^{\bullet+}$-^{3}(A$^{\bullet-}$]-R$^{\bullet}$) because the spin flip-flop ^{1}[D$^{\bullet+}$-^{3}(A$^{\bullet-}$]-R$^{\bullet}$) → ^{3}[D$^{\bullet+}$-^{1}(A$^{\bullet-}$]-R$^{\bullet}$) must occur before ^{3}[D$^{\bullet+}$-^{1}(A$^{\bullet-}$]-R$^{\bullet}$) → D$^{\bullet+}$-A-R^{-} can proceed (Figure 1). As a result, we indeed observe emissive EPR signals from both D$^{\bullet+}$ and R$^{\bullet}$ (Figure 5b), suggesting that the spin flip-flop yields an emissive hyperpolarized R$^{\bullet}$. Following reduction of R$^{\bullet}$ to R^{-}, the remaining paramagnetic species D$^{\bullet+}$ also displays an emissive polarization,[48] accounting for the observed emissive contribution convolved with the D$^{\bullet+}$ Rabi oscillations (Figure 4c).

Given the behavior of the triplet subensemble alone, a second experiment was designed to differentiate ^{1}[D$^{\bullet+}$-^{1}(A$^{\bullet-}$]-R$^{\bullet}$) and ^{1}[D$^{\bullet+}$-^{3}(A$^{\bullet-}$]-R$^{\bullet}$) during their simultaneous EPR detection using spectral hole burning (Figure 5c,d).[49,50] We take advantage of inhomogeneous broadening of the spins within the sample, largely attributed to different hyperfine fields experienced by the electron spins and slight variations in molecular geometries. For the singlet subensemble that undergoes teleportation, selectively saturating a portion of the inhomogeneous R$^{\bullet}$ spin subensemble prior to photoexcitation renders the selected spins EPR-silent, while the signal from the remaining spins is still subject to population depletion should the R$^{\bullet}$ → R^{-} electron transfer occur. This is likely not the case if a spin flip-flop takes place, since the hyperpolarization due to this process should depend on the couplings between pairs of spins, irrespective of the initial state of the individual spin. The spectral hole, burned using a narrow-bandwidth microwave pulse with a $\sim 5\pi$ turning angle, can be fit approximately with a Lorentzian line shape (Figure S8b). The delay between the hole-burning and Hahn-echo detection pulses was fixed at 10 μs, while the delay between the laser pulse and the detection pulses (τ_{DAF}) was varied. The recovery from hole burning is determined primarily by the spin−lattice relaxation time T_1, which is on the order of milliseconds for R$^{\bullet}$.[51] Therefore, the hole depth is effectively held constant throughout experiments with different values of τ_{DAF}.

A formalism for spatially incoherent spin ensembles[52] can be adapted to describe the D-A-R$^{\bullet}$ electron spin teleportation system (see the Supporting Information), yielding predictions consistent with the experimental results. Specifically, at early times, an emissive signal at the same frequency as R$^{\bullet}$ was observed with a prominent hole feature (Figure 5d). The absorptive D$^{\bullet+}$ feature shown in Figure 5d is the residual of an emissive D$^{\bullet+}$ signal primarily refocused to the other quadrature detection channel because its g-tensor is highly anisotropic. The significant anisotropy also explains the lack of observable structural and/or amplitude changes in the D$^{\bullet+}$ signal due to hole burning. The good correspondence of this early time signal and the hole-burned initial state prepared before photoexcitation suggests that the process giving rise to the signal is closely related to the Bell state measurement, i.e., ^{1}[D$^{\bullet+}$-^{1}(A$^{\bullet-}$]-R$^{\bullet}$) → D$^{\bullet+}$-A-R^{-}. At longer times, the signal grows more emissive as the hole becomes less significant but does not completely disappear.

This observation can be explained using the polarization pattern of the ^{1}[D$^{\bullet+}$-^{3}(A$^{\bullet-}$]-R$^{\bullet}$) EPR signals obtained from the picket-fence pulse experiment (Figure 5a,b). At later times, the second radical reduction event follows a ^{1}[D$^{\bullet+}$-^{3}(A$^{\bullet-}$]-R$^{\bullet}$) → ^{3}[D$^{\bullet+}$-^{1}(A$^{\bullet-}$]-R$^{\bullet}$) spin flip-flop such that the spin selection rules for radical reduction are fulfilled. The Gaussian-shaped hyperpolarized R$^{\bullet}$ signal observed at later times is consistent with the spin flip-flop mechanism. This is corroborated by the net emissive nature of the D$^{\bullet+}$ spin echo that is convolved with the Rabi oscillations resulting from teleportation (Figure 4c, blue trace). From the Rabi oscillations and the hole burning experiments (Figures 4 and 5c,d), we confirm the triplet subensemble ^{1}[D$^{\bullet+}$-^{3}(A$^{\bullet-}$]-R$^{\bullet}$) does not engage in teleportation largely due to entanglement loss in ^{1}[D$^{\bullet+}$-A$^{\bullet-}$] resulting from the coherent spin state mixing.

https://doi.org/10.1021/jacs.4c04393
J. Am. Chem. Soc. 2024, 146, 20133−20140

CONCLUSIONS

We demonstrate the advantages and challenges of using an entangled electron spin pair generated by ultrafast charge transfer within a D-A-R$^{\bullet}$ molecule to teleport information from a third stable electron spin R$^{\bullet}$ to one entangled spin of the pair. In this work, we propose a mechanism for the observed entanglement loss within the D$^{\bullet+}$-A$^{\bullet-}$ spin pair, which informs on the charge transfer time scales, spin environments, and spin−spin coupling regimes critical to electron spin teleportation. In particular, we provide insights on spin dynamics at the underexplored nanometer length scale, where strong exchange interactions dominate. It is important to note that the bipartite entanglement loss we observe in this work via teleportation does not affect the global entanglement since the system can be effectively treated as closed (i.e., total spin conservation) due to the strong exchange couplings. Another effectively closed system had been explored in the context of quantum thermalization,[53] where global entanglement was sustained while local entanglement was reported to "propagate," consistent with the bipartite entanglement loss observed in our system. The D-A-R$^{\bullet}$ system is a useful testbed where electron spin information teleported within this system provides physical insights and promises interesting applications within the field of quantum information processing, especially as the scale of the system is reduced from the ensemble level toward the single-molecule limit. Therefore, it is conceivable that a molecule-based teleportation system can be envisioned to provide spin-coherent interconnects between nanoscale quantum devices.

EXPERIMENTAL SECTION

Material Synthesis and Characterization. Detailed synthetic procedures for the precursor molecule D-A-RH and its conversion into D-A-R$^{\bullet}$ are outlined in the Supporting Information. D-A-RH was characterized using ^{1}H and ^{13}C NMR as well as MALDI-TOF spectroscopies. The D-A-R$^{\bullet}$ molecule was generated immediately before use. Stable radical R$^{\bullet}$ generation was confirmed by UV−vis spectroscopy (see the Supporting Information for additional details).

Transient Absorption Spectroscopy. Low-temperature femto- and nanosecond transient absorption (fsTA/nsTA) experiments were conducted using an apparatus described previously (see the Supporting Information for additional details). The D-A-R$^{\bullet}$ molecule was generated and transferred to a glovebox, where it was redissolved in distilled PrCN that had been stored over molecular sieves and sealed in a sample apparatus consisting of two quartz windows separated by a 2 mm PTFE spacer. The sample was removed from the glovebox and placed inside a JanisVNF-100 cryostat (Lakeshore Cryotronics) coupled to a Cryo-Con32B (Cryogenics Control Systems, Inc.) temperature controller. The temperature was lowered to 85 K for the transient absorption experiments.

Electron Paramagnetic Resonance Spectroscopy. Samples dissolved in PrCN, ∼50 μL, 100 μM, were loaded into a quartz tube (2.80 mm o.d., 2.20 mm i.d.), subjected to three freeze−pump−thaw degassing cycles on a vacuum line (10^{-4} Torr), and sealed under vacuum using an oxy-hydrogen torch. Photoexcitation of the samples was performed with 7 ns, 1.8 mJ, and 417 nm pulses using the output of an optical parametric oscillator (Spectra-Physics Basi-scan), pumped with the 355 nm output of a frequency-tripled Nd:YAG laser (Spectra-Physics Quanta-Ray Lab-170). EPR measurements were made at X-band (∼9.6 GHz) using a Bruker Elexsys E680-X/W EPR spectrometer outfitted with a split ring resonator (ER4118X-MS3), which was partially overcoupled to maximize echo intensity and minimize ringing following microwave pulses. The microwave pulse sequences summarized in the Supporting Information (Table S2) were generated with a Bruker SpinJet AWG and amplified to appropriate levels with a 1 kW TWT amplifier (Applied Systems Engineering 117X). The temperature was maintained at 85 K using an Oxford Instruments CF935 continuous-flow cryostat using liquid nitrogen. Information regarding the lab-written signal processing scripts is given in the Supporting Information.

ASSOCIATED CONTENT

Supporting Information

The Supporting Information is available free of charge at https://pubs.acs.org/doi/10.1021/jacs.4c04393.

Additional optical spectra, fsTA/nsTA data, EPR data, and theory. (PDF)

AUTHOR INFORMATION

Corresponding Authors

George C. Schatz − *Department of Chemistry, Applied Physics Program, Center for Molecular Quantum Transduction, and Paula M. Trienens Institute for Sustainability and Energy, Northwestern University, Evanston, Illinois 60208-3113, United States;* orcid.org/0000-0001-5837-4740; Email: g-schatz@northwestern.edu

Matthew D. Krzyaniak − *Department of Chemistry, Center for Molecular Quantum Transduction, and Paula M. Trienens Institute for Sustainability and Energy, Northwestern University, Evanston, Illinois 60208-3113, United States;* orcid.org/0000-0002-8761-7323; Email: mdkrzyaniak@northwestern.edu

Michael R. Wasielewski − *Department of Chemistry, Applied Physics Program, Center for Molecular Quantum Transduction, and Paula M. Trienens Institute for Sustainability and Energy, Northwestern University, Evanston, Illinois 60208-3113, United States;* orcid.org/0000-0003-2920-5440; Email: m-wasielewski@northwestern.edu

Authors

Yuheng Huang − *Department of Chemistry, Center for Molecular Quantum Transduction, and Paula M. Trienens Institute for Sustainability and Energy, Northwestern University, Evanston, Illinois 60208-3113, United States*

Yunfan Qiu − *Department of Chemistry, Center for Molecular Quantum Transduction, and Paula M. Trienens Institute for Sustainability and Energy, Northwestern University, Evanston, Illinois 60208-3113, United States;* orcid.org/0000-0002-4666-1424

Ryan M. Young − *Department of Chemistry, Center for Molecular Quantum Transduction, and Paula M. Trienens Institute for Sustainability and Energy, Northwestern University, Evanston, Illinois 60208-3113, United States;* orcid.org/0000-0002-5108-0261

Complete contact information is available at: https://pubs.acs.org/10.1021/jacs.4c04393

Notes

The authors declare no competing financial interest.

ACKNOWLEDGMENTS

This work was supported by the National Science Foundation under Award No. CHE-2154627 (M.R.W., synthesis, transient optical and EPR measurements). This research was also supported as part of the Center for Molecular Quantum Transduction, an Energy Frontier Research Center funded by the U.S. Department of Energy (DOE), Office of Science,

Basic Energy Sciences (BES), under Award DE-SC0021314 (R.M.Y., transient optical measurements, G.C.S., theory, and M.D.K., EPR data analysis). ^{1}H nuclear magnetic resonance (NMR) spectroscopy, and mass spectrometry are conducted in IMSERC facilities at Northwestern University, which have received support from the Soft and Hybrid Nanotechnology Experimental (SHyNE) Resource (NSF ECCS-2025633), NSF CHE-1048773, Northwestern University, the State of Illinois, and the International Institute for Nanotechnology (IIN).

REFERENCES

(1) Pirandola, S.; Eisert, J.; Weedbrook, C.; Furusawa, A.; Braunstein, S. L. Advances in quantum teleportation. *Nat. Photonics* **2015**, *9*, 641−652.
(2) Nielsen, M. A.; Chuang, I. L. *Quantum Computation and Quantum Information: 10th Anniversary Edtion*; Cambridge University Press: Cambridge, 2010.
(3) Aliferis, P.; Leung, D. W. Computation by measurements: A unifying picture. *Phys. Rev. A* **2004**, *70*, No. 062314.
(4) Bennett, C. H.; Brassard, G.; Crépeau, C.; Jozsa, R.; Peres, A.; Wootters, W. K. Teleporting an unknown quantum state via dual classical and Einstein-Podolsky-Rosen channels. *Phys. Rev. Lett.* **1993**, *70*, 1895−1899.
(5) Wootters, W. K.; Zurek, W. H. A single quantum cannot be cloned. *Nature* **1982**, *299*, 802−803.
(6) Barrett, M. D.; Chiaverini, J.; Schaetz, T.; Britton, J.; Itano, W. M.; Jost, J. D.; Knill, E.; Langer, C.; Leibfried, D.; Ozeri, R.; Wineland, D. J. Deterministic quantum teleportation of atomic qubits. *Nature* **2004**, *429*, 737−739.
(7) Kim, Y.-H.; Kulik, S. P.; Shih, Y. Quantum teleportation of a polarization state with a complete Bell state measurement. *Phys. Rev. Lett.* **2001**, *86*, 1370−1373.
(8) Nielsen, M. A.; Knill, E.; Laflamme, R. Complete quantum teleportation using nuclear magnetic resonance. *Nature* **1998**, *396*, 52−55.
(9) Nölleke, C.; Neuzner, A.; Reiserer, A.; Hahn, C.; Rempe, G.; Ritter, S. Efficient teleportation between remote single-atom quantum memories. *Phys. Rev. Lett.* **2013**, *110*, No. 140403.
(10) Pan, J.-W.; Gasparoni, S.; Aspelmeyer, M.; Jennewein, T.; Zeilinger, A. Experimental realization of freely propagating teleported qubits. *Nature* **2003**, *421*, 721−725.
(11) Pfaff, W.; Hensen, B. J.; Bernien, H.; van Dam, S. B.; Blok, M. S.; Taminiau, T. H.; Tiggelman, M. J.; Schouten, R. N.; Markham, M.; Twitchen, D. J.; Hanson, R. Unconditional quantum teleportation between distant solid-state quantum bits. *Science* **2014**, *345*, 532−535.
(12) Sherson, J. F.; Krauter, H.; Olsson, R. K.; Julsgaard, B.; Hammerer, K.; Cirac, I.; Polzik, E. S. Quantum teleportation between light and matter. *Nature* **2006**, *443*, 557−560.
(13) Steffen, L.; Salathe, Y.; Oppliger, M.; Kurpiers, P.; Baur, M.; Lang, C.; Eichler, C.; Puebla-Hellmann, G.; Fedorov, A.; Wallraff, A. Deterministic quantum teleportation with feed-forward in a solid state system. *Nature* **2013**, *500*, 319−324.
(14) van Loock, P.; Braunstein, S. L. Unconditional teleportation of continuous-variable entanglement. *Phys. Rev. A* **1999**, *61*, No. 010302.
(15) Wang, H.; Kais, S. Entanglement and quantum phase transition in a one-dimensional system of quantum dots with disorder. *Int. J. Quantum Inf.* **2006**, *04*, 827−835.
(16) Qiao, H.; Kandel, Y. P.; Manikandan, S. K.; Jordan, A. N.; Fallahi, S.; Gardner, G. C.; Manfra, M. J.; Nichol, J. M. Conditional teleportation of quantum-dot spin states. *Nat. Commun.* **2020**, *11*, No. 3022.
(17) Kwiat, P. G.; Mattle, K.; Weinfurter, H.; Zeilinger, A.; Sergienko, A. V.; Shih, Y. New high-intensity source of polarization-entangled photon pairs. *Phys. Rev. Lett.* **1995**, *75*, 4337−4341.
(18) Graham, T. M.; Kwon, M.; Grinkemeyer, B.; Marra, Z.; Jiang, X.; Lichtman, M. T.; Sun, Y.; Ebert, M.; Saffman, M. Rydberg-mediated entanglement in a two-dimensional neutral atom qubit array. *Phys. Rev. Lett.* **2019**, *123*, No. 230501.
(19) Lee, H.-W.; Kim, J. Quantum teleportation and Bell's inequality using single-particle entanglement. *Phys. Rev. A* **2000**, *63*, No. 012305.
(20) Julsgaard, B.; Sherson, J.; Cirac, J. I.; Fiurasek, J.; Polzik, E. S. Experimental demonstration of quantum memory for light. *Nature* **2004**, *432*, 482−486.
(21) Simon, C.; Afzelius, M.; Appel, J.; Boyer de la Giroday, A.; Dewhurst, S. J.; Gisin, N.; Hu, C. Y.; Jelezko, F.; Kröll, S.; Müller, J. H.; Nunn, J.; Polzik, E. S.; Rarity, J. G.; De Riedmatten, H.; Rosenfeld, W.; Shields, A. J.; Sköld, N.; Stevenson, R. M.; Thew, R.; Walmsley, I. A.; Weber, M. C.; Weinfurter, H.; Wrachtrup, J.; Young, R. J. Quantum memories. *Eur. Phys. J. D* **2010**, *58*, 1−22.
(22) Specht, H. P.; Nölleke, C.; Reiserer, A.; Uphoff, M.; Figueroa, E.; Ritter, S.; Rempe, G. A single-atom quantum memory. *Nature* **2011**, *473*, 190−193.
(23) Calsamiglia, J.; Lütkenhaus, N. Maximum efficiency of a linear-optical Bell-state analyzer. *Appl. Phys. B* **2001**, *72*, 67−71.
(24) żukowski, M.; Zeilinger, A.; Horne, M. A.; Ekert, A. K. Event-ready-detectors" Bell experiment via entanglement swapping. *Phys. Rev. Lett.* **1993**, *71*, 4287−4290.
(25) Massar, S.; Popescu, S. Optimal extraction of information from finite quantum ensembles. *Phys. Rev. Lett.* **1995**, *74*, 1259−1263.
(26) Bužek, V.; Hillery, M. Quantum copying: Beyond the no-cloning theorem. *Phys. Rev. A* **1996**, *54*, 1844−1852.
(27) Rugg, B. K.; Krzyaniak, M. D.; Phelan, B. T.; Ratner, M. A.; Young, R. M.; Wasielewski, M. R. Photodriven quantum teleportation of an electron spin state in a covalent donor-acceptor-radical system. *Nat. Chem.* **2019**, *11*, 981−986.
(28) Bancroft, L.; Qiu, Y.; Krzyaniak, M. D.; Wasielewski, M. R. Effect of the time delay between spin state preparation and measurement on electron spin teleportation in a covalent donor−acceptor−radical system. *J. Phys. Chem. Lett.* **2022**, *13*, 156−160.
(29) Harty, T. P.; Allcock, D. T. C.; Ballance, C. J.; Guidoni, L.; Janacek, H. A.; Linke, N. M.; Stacey, D. N.; Lucas, D. M. High-fidelity preparation, gates, memory, and readout of a trapped-ion quantum bit. *Phys. Rev. Lett.* **2014**, *113*, No. 220501.
(30) Goodson, I. T. G.; Awschalom, D. D.; Babbush, R. J.; Cheuk, L. W.; Cushing, S. K.; Frank, N. L.; Freedman, D. E.; Griffin, S. M.; Hill, S. O.; Liu, H.; Perez Garcia, M.; Rubenstein, B. M.; Schelter, E. J.; Wasielewski, M. R.; Watkins, D. *Advancing Chemistry and Quantum Information Science: An Assessment of Research Opportunities at the Interface of Chemistry and Quantum Information Science in the United States*; The National Academies Press: Washington, DC, 2023.
(31) Blair, E. P.; Tóth, G.; Lent, C. S. Entanglement loss in molecular quantum-dot qubits due to interaction with the environment. *J. Phys.: Condens. Matter* **2018**, *30*, No. 195602.
(32) de Leon, N. P.; Itoh, K. M.; Kim, D.; Mehta, K. K.; Northup, T. E.; Paik, H.; Palmer, B. S.; Samarth, N.; Sangtawesin, S.; Steuerman, D. W. Materials challenges and opportunities for quantum computing hardware. *Science* **2021**, *372*, No. eabb2823.
(33) Bowman, M. K.; Maryasov, A. G. The direct dimension in pulse EPR. *Appl. Magn. Reson.* **2021**, *52*, 1041−1062.
(34) Nelson, J. N.; Zhang, J.; Zhou, J.; Rugg, B. K.; Krzyaniak, M. D.; Wasielewski, M. R. CNOT gate operation on a photogenerated molecular electron spin-qubit pair. *J. Chem. Phys.* **2020**, *152*, 014503.
(35) Hore, P. J.; Hunter, D. A.; McKie, C. D.; Hoff, A. J. Electron paramagnetic resonance of spin-correlated radical pairs in photosynthetic reactions. *Chem. Phys. Lett.* **1987**, *137*, 495−500.
(36) Closs, G. L.; Forbes, M. D. E.; Norris, J. R. Spin-polarized electron paramagnetic resonance spectra of radical pairs in micelles: Observation of electron spin-spin interactions. *J. Phys. Chem. A* **1987**, *91*, 3592−3599.
(37) Zimmt, M. B.; Dougleday, C., Jr.; Turro, N. J. Magnetic field effect on the intersystem crossing rate constants of biradicals measured by nanosecond transient uv absorption. *J. Am. Chem. Soc.* **1985**, *107*, 6726−6727.
(38) Zimmt, M. B.; Doubleday, C., Jr.; Gould, I. R.; Turro, N. J. Nanosecond flash photolysis studies of intersystem crossing rate constants in biradicals: Structural effects brought about by spin-orbit coupling. *J. Am. Chem. Soc.* **1985**, *107*, 6724−6726.

https://doi.org/10.1021/jacs.4c04393
J. Am. Chem. Soc. 2024, 146, 20133−20140

(39) Adam, W.; Froehlich, L.; Nau, W. M.; Wirz, J. Effects of symmetrical diaryl substitution on intersystem crossing in 1,3-cyclopentanediyl triplet biradicals. *J. Am. Chem. Soc.* **1993**, *115*, 9824−9825.
(40) Weiss, E. A.; Ahrens, M. J.; Sinks, L. E.; Gusev, A. V.; Ratner, M. A.; Wasielewski, M. R. Making a molecular wire: Charge and spin transport through para-phenylene oligomers. *J. Am. Chem. Soc.* **2004**, *126*, 5577−5584.
(41) Marcus, R. A. On the theory of electron-transfer reactions. VI. Unified treatment for homogeneous and electrode reactions. *J. Chem. Phys.* **1965**, *43*, 679−701.
(42) Ulstrup, J.; Jortner, J. Effect of intramolecular quantum modes on free energy relations for electron transfer reactions. *J. Chem. Phys.* **1975**, *63*, 4358−4368.
(43) Kobori, Y.; Sekiguchi, S.; Akiyama, K.; Tero-Kubota, S. Chemically induced dynamic electron polarization study on the mechanism of exchange interaction in radical ion pairs generated by photoinduced electron transfer reactions. *J. Phys. Chem. A* **1999**, *103*, 5416−5424.
(44) Mi, Q.; Chernick, E. T.; McCamant, D. W.; Weiss, E. A.; Ratner, M. A.; Wasielewski, M. R. Spin dynamics of photogenerated triradicals in fixed distance electron donor-chromophore-acceptor-tempo molecules. *J. Phys. Chem. A* **2006**, *110*, 7323−7333.
(45) Riplinger, C.; Kao, J. P. Y.; Rosen, G. M.; Kathirvelu, V.; Eaton, G. R.; Eaton, S. S.; Kutateladze, A.; Neese, F. Interaction of radical pairs through-bond and through-space: Scope and limitations of the point-dipole approximation in electron paramagnetic resonance spectroscopy. *J. Am. Chem. Soc.* **2009**, *131*, 10092−10106.
(46) Kandrashkin, Y. E. Influence of spin decoherence on the yield of photodriven quantum teleportation in molecular triads. *J. Phys. Chem. Lett.* **2021**, *12*, 6405−6410.
(47) Coffman, V.; Kundu, J.; Wootters, W. K. Distributed entanglement. *Phys. Rev. A* **2000**, *61*, No. 052306.
(48) Colvin, M. T.; Carmieli, R.; Miura, T.; Richert, S.; Gardner, D. M.; Smeigh, A. L.; Dyar, S. M.; Conron, S. M.; Ratner, M. A.; Wasielewski, M. R. Electron spin polarization transfer from photogenerated spin-correlated radical pairs to a stable radical observer spin. *J. Phys. Chem. A* **2013**, *117*, 5314−5325.
(49) Feher, G. Electron spin resonance experiments on donors in silicon. I. Electronic structure of donors by the electron nuclear double resonance technique. *Phys. Rev.* **1959**, *114*, 1219−1244.
(50) Wacker, T.; Sierra, G. A.; Schweiger, A. The concept of FID-detected hole-burning in pulsed EPR spectroscopy. *Isr. J. Chem.* **1992**, *32*, 305−322.
(51) Sato, H.; Kathirvelu, V.; Fielding, A.; Blinco, J. P.; Micallef, A. S.; Bottle, S. E.; Eaton, S. S.; Eaton, G. R. Impact of molecular size on electron spin relaxation rates of nitroxyl radicals in glassy solvents between 100 and 300 K. *Mol. Phys.* **2007**, *105*, 2137−2151.
(52) Slichter, C. P. *Principles of Magnetic Resonance*; Spring-Verlag: New York, 1990.
(53) Kaufman, A. M.; Tai, M. E.; Lukin, A.; Rispoli, M.; Schittko, R.; Preiss, P. M.; Greiner, M. Quantum thermalization through entanglement in an isolated many-body system. *Science* **2016**, *353*, 794−800.

https://doi.org/10.1021/jacs.4c04393
J. Am. Chem. Soc. 2024, 146, 20133−20140